Sensors and Materials, Vol. 35, No. 4 (2023) 1425–1432
MYU Tokyo

S & M 3257

Electrochemical Impedance Spectroscopy of Redox Species for Ion-selective Membrane Characterization

Suthisa Leasen[1*] and Theerak Juagwon[2]

[1]Science Programme, Rajamangala University of Technology Suvarnabhumi, Bang-Kasor, Muang, Nonthaburi 11000, Thailand
[2]Materials Science and Engineering Program, Faculty of Science, Mahidol University, Thung Phyathai, Ratchadevi, Bangkok 10400, Thailand

(Received October 1, 2021; accepted March 27, 2023)

Keywords: ion-selective membrane, electrochemical impedance spectroscopy, potassium-ion-selective membrane, atomic force microscopy, ionophore

Ion-selective membranes are widely used as sensing materials in many diagnostic fields such as the pharmaceutical, environmental, and industrial fields. Ion-selective membranes are normally constructed from a neutral polymer such as polyvinyl chloride and allow ion transportation to occur through the crown structure of ionophores. To characterize the functionality of the membranes after prolonged exposure to solutions of various interfering ions, electrochemical impedance spectroscopy is utilized to investigate membrane performance, and the results are compared with those obtained from atomic force microscopy. In this study, the pore size of a membrane is quantified by using a pore size model and compared with the separation between adjacent corrugations in the profile line obtained from atomic force spectroscopy images by using image processing software.

1. Introduction

Ion-selective membranes on solid-state devices have been utilized in many research fields, for example, pharmaceutical diagnostics,(1) food quality control, and environmental monitoring, owing to their simple handling and low-cost monitoring system.(2) There are several types of ion-selective membranes with different preparation techniques and different interactions with the primary ion in the target solution. Normally, the low-molecular-weight thermoplastic polyvinyl chloride (PVC) has been employed as a scaffold for ionophores or as a structure for primary ion capture. An ion-selective membrane has a wide operation range of the primary ion concentration, usually ranging from 10^{-5} to 10^{-1} M. The important characteristics of membrane performance are a linear response to primary ions and a low selectivity coefficient over various interfering ions. These properties can be investigated via potentiometric measurement when the ion-selective membrane is exposed to the primary ions. Electrochemical impedance spectroscopy (EIS) is more suitable than potentiometric measurement for observing the membrane performance. It can be used to investigate the pore size of a membrane by immersing the

*Corresponding author: e-mail: suthisa.l@rmutsb.ac.th
https://doi.org/10.18494/SAM3674

ISSN 0914-4935

membrane in a working solution. The membrane pore size can be interpreted as the sensitivity of the membrane to the primary ions, which determines the functionality of the membrane.[3] Atomic force microscopy (AFM) is another powerful technique for pore size evaluation.[3]

Surface morphology can be observed and characterized by several techniques using the concept of the atomic or ionic interaction between the probe and atoms on the surface. AFM, which is based on an atomic interaction, is often used to investigate surface morphology. Another useful technique is EIS, which is used to obtain electrochemical images of substances with a heterogeneous surface morphology. Because EIS can determine the pore size of a membrane and AFM can observe the surface morphology through the atomic interaction, in this study, morphological images of an ion-selective membrane obtained by these two characterization techniques are investigated and compared to evaluate the membrane performance. In addition, the potentiometric signals of primary ions and ions subjected to interference are revealed.

The principle of EIS is based on applying a small-amplitude sinusoidal potential through an electrochemical system between working and reference electrodes and measuring the current from the system response, which is related to the dielectric properties of materials such as conducting polymers,[4,5] ion-selective membranes,[6–10] protective corrosion layers,[11] and biochemical substances.[12,13] The electrochemical system reveals impedance characteristics via the total impedance and the phase shift between the applied potential and the measured current. Hence, the real impedance can be plotted against its imaginary counterpart (Nyquist plot) or the frequency can be plotted against the phase shift (Bode plot) for electrical quantification. According to the pore size model, the changes in transition frequency correspond to the pore diameter when the frequency band is applied to the porous dielectric materials, which is described as a waveguide size.

In this study, the pore size of an ion-selective membrane was determined from images obtained from high-performance AFM and EIS systems. The AFM data was compared with the active radius obtained from by EIS, which is governed by the pore size model. EIS revealed significant surface damage via an increase in electroactive domain radius, and AFM was able to determine a reasonable pore radius of the membrane.

2. Materials and Methods

2.1 Apparatus and reagents

First, the ion-selective membrane must perform its function of responding to the primary ion. For this reason, the performance of the membrane was evaluated by potentiometry while applying a constant voltage (approximately 1.54 V versus a AgCl pseudo-reference electrode) to an ion-selective field-effect transistor (ISFET; Winsense Co., Ltd.) coated with a nitrate-ion-selective membrane. Then, the concentration of the primary and interfering ions was decreased from 0.10 M to 1 mM.

The EIS of the nitrate-ion-selective membrane was carried out using a PalmSens3 frequency response analyzer with a fixed potential mode at 0.19 V versus Ag/AgCl (the standard potential

of ferri/ferrocyanide) coupled with a sine wave of 10 mV amplitude in the presence and absence of nitrate ions associated with $Fe[CN_6]^{3-/4-}$ redox species. The operating system was composed of three electrodes in one compartment cell: a membrane-coated semiconducting solid substrate as a working electrode, Ag/AgCl as a reference electrode, and a Pt rod as a counter electrode. To maintain the organic crown structure of the ionophore, Tris-HCl (pH 7) was used as a supporting electrolyte for this system. The EIS spectra were analyzed using the EIS spectrum analyzer freeware.

The tapping mode of the AFM system was used to observe the surface morphology of bare indium oxide–doped tin (ITO) and ion-selective-membrane-coated indium oxide–doped tin (Mem/ITO). A NanoScope IV operating system (Veeco Metrology Group, Scientific and Technological Research Equipment Center, Chulalongkorn University) was used for this observation. A raster probe was scanned over an area of 1 μm^2 of each sample. The surface roughness R_a and RMS of each sample were characterized using Gwyddion software. The membrane pore size was directly measured from the profile line.

PVC was purchased from Sigma-Aldrich. Tetrahydrofuran (THF) and sodium chloride were obtained from Labscan. Bis(2-ethylhexyl)sebacate, magnesium chloride, potassium tetrakis(4-chlorophenyl)borate, and nitrate ionophore VI were purchased from Fluka. Potassium nitrate was obtained from BDH Chemicals. All potentiometry and stock solutions were prepared in de-ionized water obtained from the Division of Chemistry, Department of Science, Faculty of Science and Technology, Rajamangala University of Technology Suvarnabhumi.

2.2 Preparation of functionalized PVC membrane

The functionalized membrane comprised PVC, plasticizer [bis(2-ethylhexyl)sebacate)], ion excluder [potassium tetrakis(4-chlorophenyl)borate], and nitrate ionophore. First, 33 mg of PVC was vigorously stirred in 1.50 ml of THF, then 32 µl of plasticizer, 1.50 mg of ion excluder, and 2 mg of nitrate ionophore were added (Fig. 1). After the mixture was homogenized, the

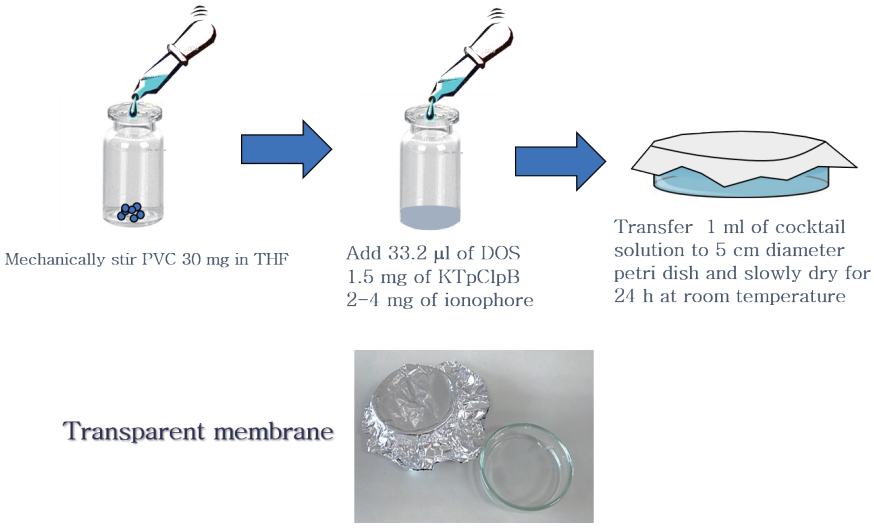

Fig. 1. (Color online) Experimental setup used in this study.

suspension was rinsed in a 5-cm-diameter Petri dish. Then, THF was slowly dried at room temperature overnight. The usable nitrate-selective membrane appeared as a clear sticky film.

3. Results and Discussion

3.1 Response of ion-selective membrane

First, the naked ISFET was calibrated through pH calibration so that it exhibited Nernstian behavior with a slope close to 60 mV pH^{-1}. Then, the ISFET was covered by a nitrate-ion-selective membrane to test the selectivity of the membrane and to observe interfering ions such as chloride ions. It was found that chloride ions can suppress the selectivity of the nitrate membrane, indicating its partial selectivity. As shown in Fig. 2, the chloride ions gave a Nernstian slope of −77 $mVdec^{-1}$ for the nitrate-selective membrane, whereas the slope for the nitrate primary ions was −79 $mVdec^{-1}$. [14] These slopes reveal the strong interference of chloride ions with the nitrate-ion-selective membrane. The similar radii of these two ions allow chloride ions to compete with nitrate ions in occupying the ion-sensing structure of the membrane.

3.2 Surface morphology

The surface morphology of bare ITO [Fig. 3(a)] comprises small grains, corresponding to the crystalline structure of the semiconductor surface. After coating the ion-selective membrane [Fig. 3(b)], the grain boundary of ITO was replaced by the pore structure of the membrane. Using image processing freeware, the pore size of the membrane was quantified by measuring the full width at half maximum of each pore structure. According to this approximation, the membrane pore diameter was 5.2 ± 1.4 nm, consistent with the normal pore size of an ion-selective membrane.[12,15]

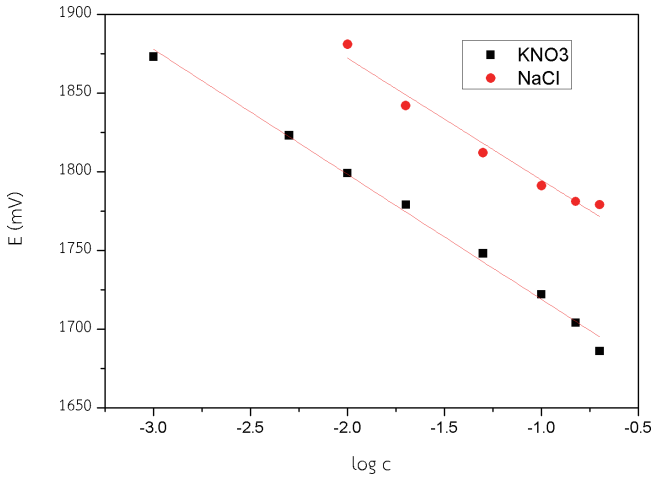

Fig. 2. (Color online) Responses of nitrate-ion-selective membrane to NO^{3-} and Cl^{-}.

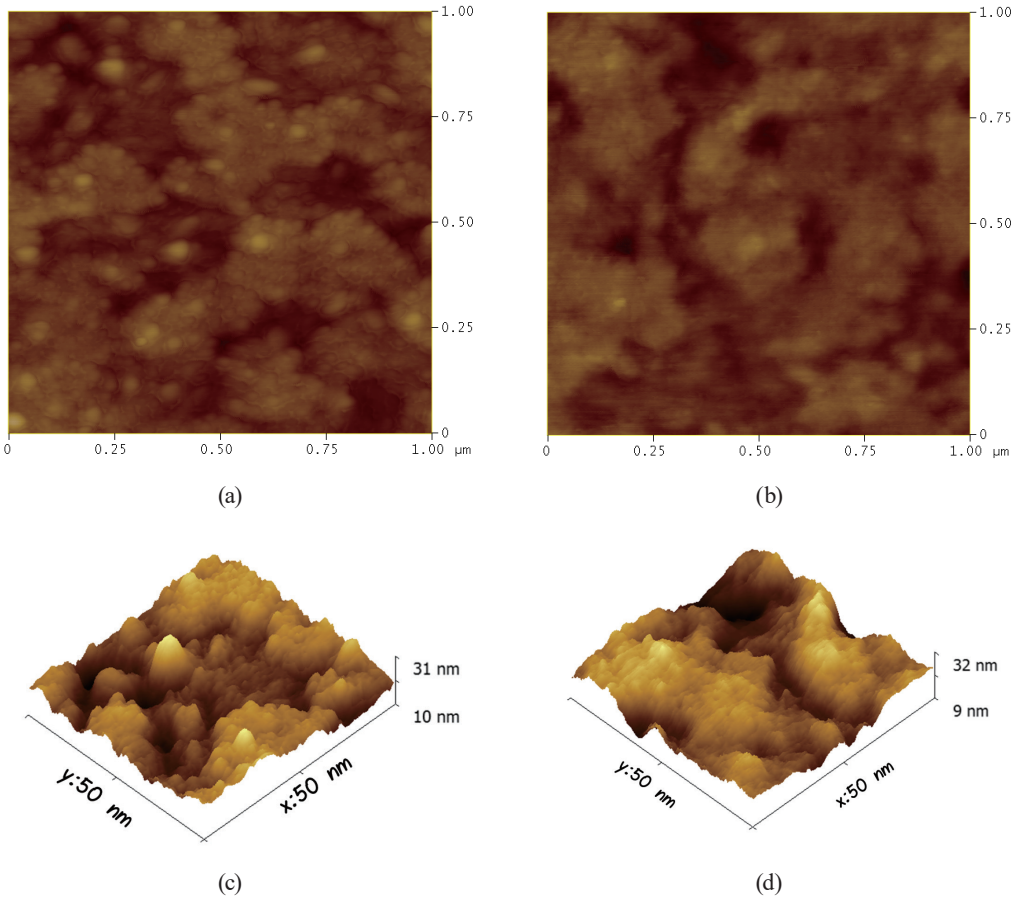

Fig. 3. (Color online) Surface morphologies of (a, c) ITO and (b, d) nitrate-ion-selective membrane over equivalent total scan area of 1 μm × 1 μm.

3.3 Transition frequency of nitrate-ion-selective membrane

EIS spectra normally represent the electrochemical system at the surface of an electrode via a Nyquist plot, in which the real part of the impedance is plotted against the imaginary part to explain the electrical component of the interface between the electrode and the solution, especially ions adhering to the surface. Therefore, the electrochemical impedance spectra revealed, via an equivalent circuit, the electrochemical phenomena due to the interaction between the ion-selective membrane and ions adhering to the surface and in the bulk. To calculate the diffusion coefficient of a redox species in any supporting electrolyte, the real part of impedance is plotted against the inverse square root of the angular frequency as shown in Fig. 4. Both the ITO electrode (black squares) and the ion-selective-membrane-coated ITO electrode (red circles) exhibit a straight line in the low-frequency range, indicating that the majority behavior of ions is diffusion. The semicircular part of the impedance spectra in Fig. 4 in the low-frequency range indicates the porous structure of the insulator on the conducting surface. Furthermore, the straight lines in the high-frequency range indicate that redox species

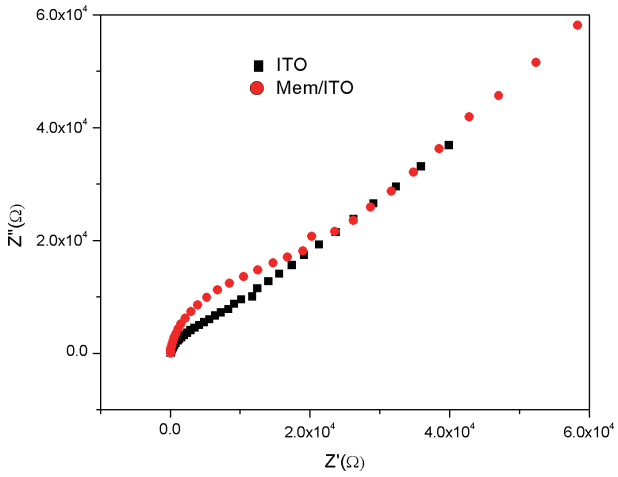

Fig. 4. (Color online) Nyquist plot of ITO (■) and nitrate-ion-selective-membrane-coated ITO (●) in Tris-HCl:NaCl (10:1) at pH 7.0 using 100 µM of $[Fe(CN)_6]^{4-/3-}$ as redox species and 50 mM of NO^{3-}.

diffused to the ITO and Mem/ITO surfaces in the same manner. This means that ions could diffuse to the ITO and Mem/ITO surfaces in the same manner owing to their similar pore sizes and intervals between adjacent pores. The calculated slope gives the diffusion coefficient of $[Fe(CN)_6]^{4-/3-}$ in the Tris-HCl supporting electrolyte of 8.35×10^{-8} cm^2s^{-1}. Using this value, the pore radius r_a and the distance between pores in the membrane, r_b, of the pinhole were evaluated. As shown in Fig. 5, the porous surface produces a sharp peak called the transition frequency, which corresponds to the highest imaginary part of impedance in the high-frequency range.

3.4 Pore radius for various primary ion concentrations

According to the pore size model,[13] the porous surface of the membrane can be considered as a cylindrical waveguide. The uncovered dielectric material of ITO had the radius r_a and pore separation distance r_b. At the low primary ion concentration of 10 µM, r_a was 24 ± 1 nm and r_b was 49 ± 3 nm for the membrane. When the primary ion concentration was increased to 50 and 100 µM, r_a decreased to 14 ± 6 and 21 ± 2 nm, respectively. These pore sizes were determined from the pore size model using the transition frequency corresponding to the peak in Fig. 5. The increase or decrease in pore size should depend on the number of ion sites in a membrane. At low primary ion and interfering ion concentrations of 10 to 100 µM, chloride ions can compete with nitrate ions, hence both chloride and nitrate ions diffused into the membrane. Accordingly, in Fig. 6, all three concentrations, 0.01, 0.05, and 0.1 µM, gave a precise pore diameter. The pore size of the membrane obtained by EIS was double the value obtained by AFM measurement. This may be due to unoccupied ion sites resulting in the EIS spectra only representing diffusive pores.

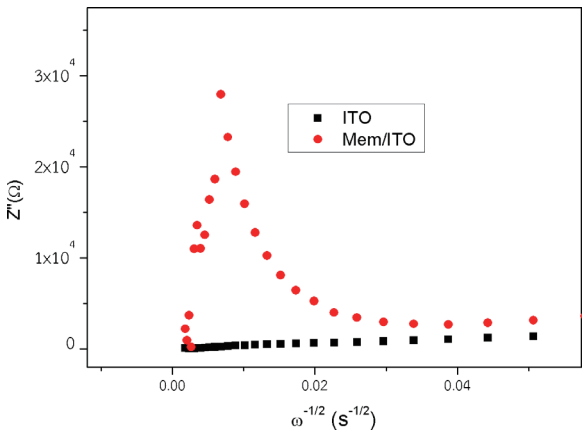

Fig. 5. (Color online) Plot of imaginary part of impedance (Z″) against square root of frequency of ITO (■) and nitrate-ion-selective-membrane-coated ITO (●) in Tris-HCl:NaCl (10:1) at pH 7.0 using 100 μM of $[Fe(CN)_6]^{4-/3-}$ as redox species with 10 μM of NO^{3-}.

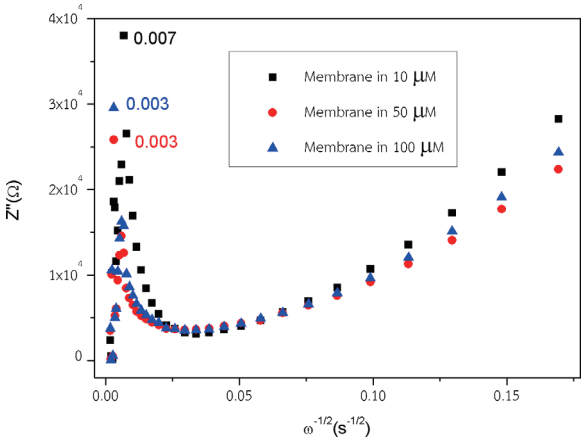

Fig. 6. (Color online) Plot of imaginary part of impedance (Z″) against square root of frequency of nitrate-ion-selective-membrane-coated ITO in Tris-HCl:NaCl (10:1) at pH 7.0 using 100 μM $[Fe(CN)_6]^{4-/3-}$ as the redox species and (■) 10, (●) 50, and (▲) 100 μM of NO^{3-}.

3.5 Effect of prolonged exposure to oxygen

After the membrane was exposed to oxygen for 3 days, its pore size increased to 68 nm, three times that of the freshly prepared membrane, and its pore separation distance increased to 137 nm. The oxygen in air can damage the organic crown structure of the ionophore, which plays an important role in capturing ions. This damage decreased the number of ion sites, resulting in an increase in distance between pores. The results show the advantageousness of EIS for the real-time investigation of the pore size of an ion-selective membrane.

4. Conclusions

In this study, an ion-selective membrane coated on a solid substrate was investigated through EIS and AFM, which operate in different environments. The pore size evaluated via EIS according to the pore size model was 49 ± 3 nm, which decreased threefold after it was exposed to oxygen, whereas AFM, which was performed in vacuum, gave a pore diameter of 5.2 ± 1.4 nm. The two techniques of AFM and EIS gave very different pore sizes of the ion-selective membrane. Therefore, further evaluation of the pore size of the ion-selective membrane in the same experimental setup is required. In comparison, the pore diameter obtained by EIS calculation was larger than that obtained by AFM calculation. The assumptions for this work were as follows: i) the pore size model is limited to very small structures and ii) the overlapping of adjacent pores is greater than the distance between them and less than the diffusion layer thickness.

Acknowledgments

This work was financially supported by the National Research Council of Thailand. We also thank Materials Science and Innovation Research Unit at Rajamangala University of Technology Suvarnabhumi for providing the workplace.

References

1 M. I. Yousry and F. K. Amal: J. Adv. Res. **2** (2011) 25. https://doi.org/10.1016/j.jare.2010.08.007
2 R. De Macro, G. Clarke, and B. Pejcic: Electroanalysis **19** (2007) 1987. https://doi.org/10.1002/elan.200703916
3 N. Hilal, L. Al-Khatib, H. Al-Zoubi, and R. Nigmatullin: Desalination **184** (2005) 45. https://doi.org/10.1016/j.desal.2005.02.071
4 D. Benito, J. J. García-Jareño, J. Navarro-Laboulais, and F. Vicent: J. Electroanal. Chem. **446** (1998) 47. https://doi.org/10.1016/S0022-0728(97)00565-2
5 R. N. Vyas and B. Wang: Int. J. Mol. Sci. **11** (2010) 1956. https://doi.org/10.3390/ijms11041956
6 V. Freger and S. Bason: J. Membr. Sci. **302** (2007) 1. https://doi.org/10.1016/j.memsci.2007.06.046
7 K. N. Mikhelson: Chem. Anal. (Warsaw) **51** (2006) 853.
8 A. Radu, S. Anatasova-Ivanova, B. Paczosa-Bator, M. Danielewski, J. Bobacka, A. Lewenstam, and D. Diamond: Anal. Methods. **2** (2010) 1490. https://doi.org/10.1039/C0AY00249F
9 C. R. Magaña-Zavala, M. E. Angelels-San Martin, F. J. Rodríguez-Gómez, D. R. Acosta, R. Ávila-Godoy, and B. Hidalgo-Prada: Anti-Corros. Methods Mater. **57** (2010) 118. https://doi.org/10.1108/00035591011040074
10 A. Lisowska-Oleksiak, U. Lesińska, A. P. Nowak, and M. Bocheńska: Electrochim. Acta **51** (2006) 2120. http://doi.org/10.1016/j.electacta.2005.04.078
11 C. Simpliciano, L. Clark, B. Asi, N. Chu, M. Mercado, S. Diaz, M. Goedert, and M. Mobed-Miremadi: J. Surf. Eng. Mater. Adv. Technol. **3** (2013) 1. https://doi.org/10.4236/jsemat.2013.34A1001
12 C. Susana, M. Pedrero, C. Montemayor, E. Fatás, and J. M. Pingarrón: J. Electroanal. Chem. **586** (2006) 112. https://doi.org/10.1016/j.jelechem.2005.09.007
13 M. Mazloum-Ardakani, A. D. Manshadi, S. A. Mozaffari, and H. Azizi: Iranian J. Math. Chem. **4** (2013) 41. https://doi.org/10.22052/IJMC.2013.5281
14 M.-H. Piao, J.-H. Yoon, G. Jeon, and Y.-B. Shim: Sensors **3** (2003) 192. https://doi.org/10.3390/s30600192
15 M. M. Khaydukova, O. A. Zadorozhnaya, D. O. Kirsanov, H. Iken, D. Rolka, M. Schöning, V. A. Babain, Y. G. Vlasov, and A. V. Legin: Russ. J. Appl. Chem. **87** (2014) 307. https://doi.org/10.1134/S1070427214030112

About the Authors

Suthisa Leasen received her B.S. degree from Kasetsart University, Thailand, in 2005 and her Ph.D. degree from Mahidol University, Thailand, in 2012. Since 2018, she has worked for the Materials Science and Innovation Research Unit of Rajamangala University of Technology Suvarnabhumi. Her research interests are in electrochemical biosensors, ion-selective electrodes, and surface characterizations. (suthisa.l@rmutsb.ac.th)

Theerak Juagwon received his B.S. degree from Prince of Songkhla University, Thailand, in 2008 and his M.S. and Ph.D. degrees from Mahidol University, Thailand, in 2012 and 2019, respectively. His research interests are in organic semiconductors, optical and electrochemical sensors based on organic molecules, and metal oxides and their applications.
(t.juagwon@gmail.com)